V European Conference on Computational Fluid Dynamics
ECCOMAS CFD 2010
J. C. F. Pereira and A. Sequeira (Eds)
Lisbon, Portugal,14-17 June 2010

# LES OF AIRCRAFT WAKE VORTICES EVOLVING IN A STABLY STRATIFIED AND WEAKLY TURBULENT ATMOSPHERE

**I. De Visscher, L. Bricteux and G. Winckelmans**

Université catholique de Louvain (UCL),
Institute of Mechanics, Materials and Civil engineering (iMMC),
Bât. Stévin, Place du Levant, 2
B-1348 Louvain-La-Neuve, Belgium
e-mail: ivan.devisscher@uclouvain.be

**Key words:** LES, aircraft wake vortices, stratification, turbulent atmosphere

**Abstract.** *The aim of this study is to investigate the influence of weakly turbulent stable stratification of the atmosphere on aircraft wake vortex behavior, by means of Large Eddy Simulations (LES). In order to best represent the atmospheric conditions, the stratified and weakly turbulent fields are here first generated, using LES of forced and stratified turbulence. The obtained fields are non-isotropic. LES of a pair of counter rotating vortices, with relatively tight cores, evolving in the obtained fields are then performed. Different stratification levels are investigated, from low to very high, and all with weak turbulence. The simulations are performed at very high Reynolds number; much higher than in previous work, thus more realistic. The current investigation is performed using a pseudo-spectral code with various subgrid scale (SGS) models. The influence of the domain size is also investigated, with box sizes also allowing the Crow instability development. The chosen resolution ensures that the essential dynamics of the vortices is properly captured. The time evolution of the wake vortex characteristics (positions and circulation) are studied as a function of the stratification level. They are also compared to those obtained from previous simulations performed with stratification but without turbulence. It also appears that the turbulence of the temperature field has a strong impact on the decay of the vortices. It enhances the development of 3-D instabilities in the baroclinic vorticity. Hence, this quickens its interaction with the primary vortices, leading to a fast decay. A simplified model of altitude evolution is also proposed and fitted on the present results. Such model can be used in operational models for predicting the wake vortex behavior (transport and decay).*

## 1 INTRODUCTION

As a consequence of its lift, an aircraft generates a wake that eventually forms a pair of counter-rotating vortices with circulation $\Gamma_0$ and $-\Gamma_0$, and separated by a distance $b_0$, that sink under their mutual influence. It has been shown, in previous numerical studies[1,2,3,4], that the thermal stratification induces a deceleration of the vortex descent rate, and that it also significantly enhances the wake circulation decay.

The aim of this investigation is to address the influence of the atmosphere stable stratification on the wake vortex behavior (position and circulation). This is of major interest to Air Traffic Management (ATM) as the strong rolling moment induced by those wake vortices on a following aircraft entering the wake can be hazardous.

For that purpose, Large Eddy Simulations (LES) of wake vortices, at very high Reynolds number, are performed with various stratification levels. In order to investigate the influence of the atmospheric conditions, stratified turbulent fields are generated and supplemented to the two-vortex system. These fields are three-dimensional, non-isotropic, unsteady and turbulent, so that prior LES are required to generate them.

The results of this investigation will also be used to further improve and calibrate operational models for predicting the wake vortex behavior (transport and decay). Since the stratification has a strong impact on wake vortex transport and decay, a good real-time modeling of the phenomenon is indeed of primary importance.

## 2 GOVERNING EQUATIONS AND NUMERICAL METHOD

The governing equations are the Navier-Stokes equations for incompressible flows, using the Boussinesq approximation, and supplemented by a subgrid scale (SGS) model:

$$\nabla \cdot \mathbf{u} = 0 \tag{1}$$

$$\frac{\partial \mathbf{u}}{\partial t} + (\mathbf{u} \cdot \nabla)\,\mathbf{u} = -\nabla P + \nu \nabla^2 \mathbf{u} + \nabla \cdot \boldsymbol{\tau}^M + g\,\beta\,\tilde{\Theta}\,\mathbf{e}_z \tag{2}$$

$$\frac{\partial \tilde{\Theta}}{\partial t} + (\mathbf{u} \cdot \nabla)\,\tilde{\Theta} + w \frac{d\bar{\Theta}}{dz} = \alpha \nabla^2 \tilde{\Theta} - \nabla \cdot \boldsymbol{q}^M \tag{3}$$

where $\mathbf{u} = (u, v, w)$ is the LES velocity field, $P = \frac{p}{\rho}$ the reduced pressure, $\nu$ the kinematic viscosity, $\boldsymbol{\tau}^M$ the SGS stress tensor model, $g$ the acceleration due to gravity, $\beta$ the thermal expansion coefficient, $\alpha$ the thermal diffusivity and $\boldsymbol{q}^M$ the SGS heat flux model.

The potential temperature $\Theta$ has here been decomposed into the mean vertical profile and the deviation around this mean:

$$\Theta(\mathbf{x}, t) = \bar{\Theta}(z) + \tilde{\Theta}(\mathbf{x}, t), \tag{4}$$

with $\frac{d\bar{\Theta}}{dz}$ constant. This enables to perform the simulations in a periodic domain.

### 2.1 Pseudo-spectral Navier-Stokes solver

The Navier-Stokes solver considered here is based on the Fourier-Galerkin pseudo-spectral methodology. The spectral approximation of the velocity vector $\boldsymbol{u}$ is symbolically written as

$$\boldsymbol{u}(\boldsymbol{x},t) = \sum_{\boldsymbol{k}} \widehat{\boldsymbol{u}}(\boldsymbol{k},t)\ \exp(\, i\, \boldsymbol{k}\cdot\boldsymbol{x}\,), \tag{5}$$

where the spatial wavenumber vector is $\boldsymbol{k} = (\, k_x,\, k_y,\, k_z)$. The " $\widehat{\cdot}$ " notation is used to identify Fourier transforms.

The time integration of equations (2) and (3) are carried out in spectral space using a technique in which the convective and SGS model terms are marched explicitly using the 3rd order Williamson scheme. The nonlinear terms are evaluated using a pseudo-spectral algorithm and the dealiasing is done using a phase shift procedure[5]. The incompressibility constraint (i.e., the effect of $\nabla P$), Eq. (1), is satisfied by reprojection of the velocity field into a divergence free space.

### 2.2 High order hyperviscosity SGS model

The hyperviscosity formulation used in this study provides a SGS dissipation term acting solely at the small scales of the LES grid, without affecting the large to medium scale dynamics. The SGS model is taken as:

$$\tau_{ij}^{M} = (-1)^p\, \nabla^{2p}\, (2\nu_h S_{ij})\ . \tag{6}$$

We here use a constant $\nu_h$ (i.e., a linear model) where

$$\nu_h = \frac{1}{T_0} C^{(p)} h^{2(p+1)}\,, \tag{7}$$

$T_0$ being a global time scale. One then obtains, in spectral space:

$$\widehat{\nabla\cdot\boldsymbol{\tau}^{M}}(\mathbf{k}) = (-1)^p\, \nu_h\, (|\boldsymbol{k}|)^{2(p+1)}\, \widehat{\boldsymbol{u}}(\boldsymbol{k})\,. \tag{8}$$

In a similar way, we have:

$$\widehat{\nabla\cdot\boldsymbol{q}^{M}}(\mathbf{k}) = (-1)^p\, \alpha_h\, (|\boldsymbol{k}|)^{2(p+1)}\, \widehat{\Theta}(\boldsymbol{k})\,. \tag{9}$$

In the present work, we used $p = 7$ and $Pr_h = \frac{\nu_h}{\alpha_h} = 1$. The molecular viscosity is set to zero as the Reynolds number is very high. Previous studies[6,7] showed that this model performs well for LES of aircraft wake vortex flows. Indeed hyperviscosity models preserve the large scale dynamics as they dissipates kinetic energy on a narrow range at the highest wavenumbers.

### 2.3 Regularized variational multiscale SGS model

The regularized variational multiscale (RVM) models[8] use the high-pass filtered (HPF) velocity field $\boldsymbol{u}^s$ which is computed from the difference between the LES velocity field, $\mathbf{u}$, and the low-pass filtered field, $\overline{\boldsymbol{u}}^{(n)}$ obtained using a higher order (order $2n$) filter.

$$\boldsymbol{u}^{s^{(n)}} = \boldsymbol{u} - \overline{\boldsymbol{u}}^{(n)} \tag{10}$$

In Fourier space, the obtained filtered field is

$$\begin{aligned} \widehat{\overline{\boldsymbol{u}}}^{(n)}(\mathbf{k}) &= G^{(n)}(k_x h)\, G^{(n)}(k_y h)\, G^{(n)}(k_z h)\, \widehat{\boldsymbol{u}}(\mathbf{k}) \\ &= \left(1 - \sin^{2n}\left(k_x \Delta/2\right)\right) \\ &\quad \left(1 - \sin^{2n}\left(k_y \Delta/2\right)\right) \\ &\quad \left(1 - \sin^{2n}\left(k_z \Delta/2\right)\right) \widehat{\boldsymbol{u}}(\mathbf{k})\,. \end{aligned} \tag{11}$$

The RVM model is then taken as

$$\tau_{ij}^M = 2\nu_{sgs}\, S_{ij}^s\,, \tag{12}$$

where $S_{ij}^s$ is the strain rate tensor of the HPF field (written in physical space but computed in Fourier space):

$$S_{ij}^s = \frac{1}{2}\left(\frac{\partial u_i^s}{\partial x_j} + \frac{\partial u_j^s}{\partial x_i}\right)\,. \tag{13}$$

This means that the SGS model only acts on the small scale content of the LES field thus preserving the dynamics of the large scales. Here, we consider the subclass of RVM models, noted RVMs, where the SGS viscosity is itself computed using the HPF field (small scale content of the LES field):

$$\nu_{sgs} = \nu_{sgs}^s = C\,\Delta^2\left(2\,S_{ij}^s S_{ij}^s\right)^{1/2}\,. \tag{14}$$

The model coefficient has been calibrated[9] to $C = 0.11$ with $n = 3$. Concerning the SGS heat flux model, $\boldsymbol{q}^M$, it is defined as:

$$\boldsymbol{q}^M = -\alpha_{sgs}\,\frac{\partial \widetilde{\Theta}^s}{\partial x_i}\,. \tag{15}$$

The SGS thermal diffusivity $\alpha_{sgs}$ is chosen so that $Pr_{sgs} = \frac{\nu_{sgs}}{\alpha_{sgs}} = 1.0$.

This model triggers only when small scales appear in the flow. This is an interesting feature as the model is inactive in laminar parts of the flow, e.g. in the core of a vortex. It has been shown[9] that the RVM models with high order filtering, can produce a significant inertial subrange in homogeneous isotropic turbulence and thus capture well the turbulence physics. This is because they have a sufficient range of wavenumbers preserved from any SGS dissipation. The RVMs model has also been used successfully to simulate a four vortex system flow[10]. For these reasons, the RVMs model is particularly well suited for LES of aircraft wake vortex flows.

## 3 NUMERICAL SET-UP

The initial wake vortex flow is composed of a pair of vortices of circulation $\Gamma_0$ and $-\Gamma_0$, and separated by a distance $b_0$. A low order algebraic velocity profile was used for each vortex:

$$\Gamma(r) = \Gamma_0 \frac{r^2}{(r^2 + r_c^2)},\ u_\theta(r) = \frac{\Gamma(r)}{2\,\pi\,r}, \tag{16}$$

where $r_c$ is the radius of maximum tangential velocity: it was here set to $r_c = 0.05\,b_0$ (which is fairly realistic for aircraft wake vortices after roll-up with values between 0.03 and 0.05). The vortex pair sinks initially at a velocity $V_0$, also leading to the definition of a characteristic time $t_0$,

$$V_0 = \frac{\Gamma_0}{2\,\pi\,b_0},\ t_0 = \frac{b_0}{V_0}\,. \tag{17}$$

The stable stratification level is characterized by the Brunt-Väisälä frequency, $N$, defined by:

$$N^2 = \frac{g}{\Theta_0}\frac{d\bar{\Theta}}{dz}, \tag{18}$$

where $\Theta_0$ is the reference potential temperature. In a dimensionless form, this leads to

$$N^* = N\,t_0\,. \tag{19}$$

Five simulations have been performed using different stratification levels: $N^* = 0.0$, 0.35, 0.75, 1.0 and 1.4. The Reynolds number of the flow, $Re_\Gamma = \frac{\Gamma_0}{\nu}$, is very high so that we here perform LES "in the limit of very high Reynolds number", where any molecular viscosity effect can be neglected.

The periodicity lengths are set to $L_x \times L_y \times L_z = 4\,b_0 \times 4\,b_0 \times 4\,b_0$ using $256^3$ grid points. The extension in the $y$ and $z$ directions limits the influence of the periodicity and enables to obtain valid results for large times. The numerical resolution is $\frac{h}{b_0} = \frac{1}{64}$, which ensures that the dynamic of the vortices is properly captured ($r_c/h \geq 3$).

In order to simulate the wake vortices in realistic stratified conditions, for each stratification level, stratified turbulent fields are first generated. For that purpose, we perform LES of forced stratified turbulence. The field are obtained by forcing the low wave numbers of the flow with a certain forcing $\left(\frac{dE}{dt}\right)_f$ and by letting the stratified turbulence evolve until it reaches a statistically converged state (based on energy and dissipation evolutions). The chosen energy forcing level is set to:

$$\left(\frac{dE}{dt}\right)_f^* = \left(\frac{dE}{dt}\right)_f \frac{b_0}{V_0^3} = 2.4\,10^{-4} \tag{20}$$

For an unstratified atmosphere at equilibrium, the forcing will be equal to the eddy dissipation rate $\epsilon$. For vortices generated by a large aircraft with $b_0 = 50$ m and $\Gamma_0 = 400$ m$^2$/s, $\epsilon^* = 2.4\,10^{-4}$ would then correspond to an eddy dissipation rate $\epsilon = 10^{-5}$ m$^2$/s$^3$,

which indeed corresponds to a calm atmosphere. For each $N^*$ value, once the stratified turbulence has reached its own equilibrium, the wake vortex field is supplemented to the obtained LES field.

## 4 RESULTS

The results are presented in a dimensionless form, using $b_0$, $\Gamma_0$, $V_0$ and $t_0$ for characteristic length, circulation, velocity and time, respectively. The dimensionless time is $\tau = \frac{t}{t_0}$.

### 4.1 Flow visualization

We provide, in Fig. 1, a visualization of the flow, using iso-surfaces of the $\lambda_2$ criterion[11], for the case with $N^* = 1.0$. At $\tau = 0.5$, one observes the two vortex cores; the wake vortices descent at a constant speed and the initial separation stays constant (as it will be further quantified hereafter).

Due to the vertical mean temperature gradient $\frac{d\bar{\Theta}}{dz}$, local warm and cold zones are formed around the wake vortices. This leads to the creation of local gradients of temperature in the axial, $x$, and lateral, $y$, directions. Those gradients are sources of production of vorticity, called baroclinic vorticity.

For $\tau \geq 1.0$, the production of this baroclinic vorticity, of opposite sign, leads to the formation of coherent transverse vortical structures. This production is confined in the Rankine oval of the vortex system. It is important to note that since the background temperature field is turbulent, the baroclinic vorticity is also directly turbulent when created. These secondary structures are subjected to short waves instabilities which grow in time ($\tau = 1.5$). These instabilities keep growing, eventually leading to a complex turbulent vortex system. At $\tau = 1.75$, the primary vortices are still coherent and surrounded by a cloud of secondary turbulent vorticity. For $\tau \geq 1.75$, the strong 3-D interaction between this secondary vorticity and the primary vortices leads to a fast decay of the primary vortex circulation (as further quantified). At late stages of the flow development ($\tau \geq 2.0$), the flow is so complex that one can no longer distinguish the vortex cores on the 3-D visualizations. However, on the longitudinally averaged flow (i.e., a RANS mean), one can still observe mean "coherent" primary vortices.

### 4.2 Vortex trajectories

For the vortex global characterization, we compute the diagnostics on the longitudinally averaged vorticity fields:

$$\overline{\omega}(y, z, t) = \frac{1}{L_x} \int_0^{L_x} \omega(\mathbf{x}, t)\, dx\,. \tag{21}$$

The stratification effects have a strong impact on the vortex trajectory. In order to measure the mean displacement of the vortices, we compute the position of the vortex

$\tau = 0.5$

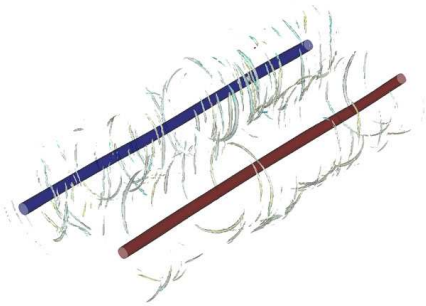

$\tau = 1.0$

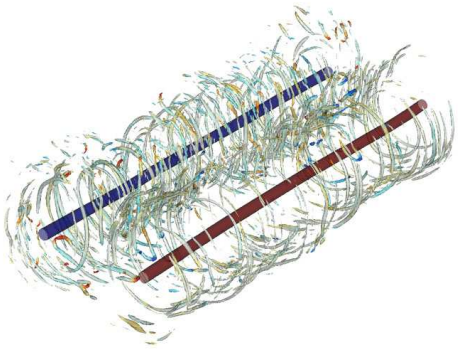

$\tau = 1.25$

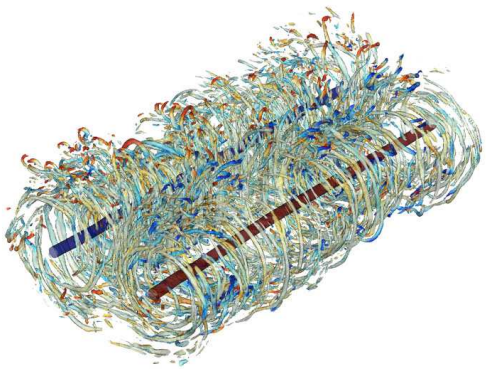

$\tau = 1.5$

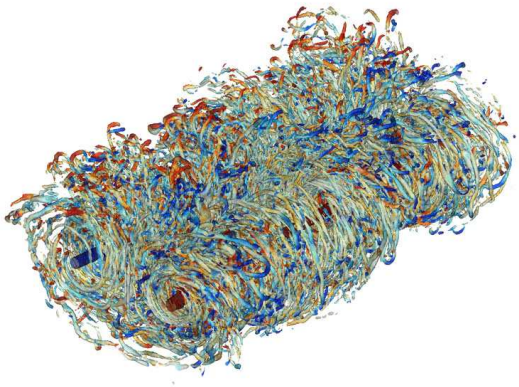

$\tau = 1.75$

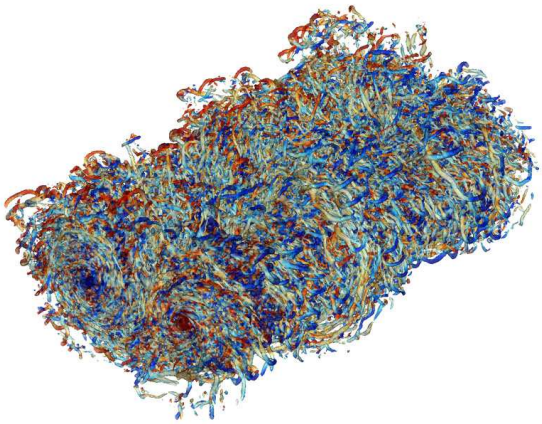

$\tau = 2.0$

Figure 1: Case $N^* = 1.0$: iso-$\lambda_2$ surfaces at different times colored by the axial vorticity $\omega_x\, b_0^2/\Gamma_0$ .

centroid, based on the axially averaged flow.

$$\overline{\Gamma} = \int_{\Omega} \overline{\omega}_x(y,z,t)\, d\Omega, \tag{22}$$

$$y_c(t) = \frac{1}{\overline{\Gamma}} \int_{\Omega} y\, \overline{\omega}_x(y,z,t)\, d\Omega, \tag{23}$$

$$z_c(t) = \frac{1}{\overline{\Gamma}} \int_{\Omega} z\, \overline{\omega}_x(y,z,t)\, d\Omega, \tag{24}$$

where $\Omega$ is a square centered on the position of the maximum (resp. minimum) of vorticity and with sides of $\frac{b_0}{4}$, for the right (resp. left) vortex, and $\overline{\Gamma}$ is the circulation evaluated on this area. In order to understand the flow mechanisms it is also interesting to measure the vortex lateral spacing defined by:

$$b_c = y_{c,right} - y_{c,left}\,. \tag{25}$$

Fig. 2 presents the altitude and lateral spacing evolution for the five considered stratification levels. As expected, the stratification level controls the time of rebound. For the case $N^* = 1.4$, the vortices are almost at the altitude of wake generation after a time $\tau = 3.0$. For large aircraft, at low altitude, $t_0 \approx 30$ s; hence, in this case, the vortices would be back to the flight altitude after 90 s, although much decayed (see later). It is also interesting to note that, for low stratification levels ($N^* = 0.35$), the lateral spacing of the vortices remains almost constant. For intermediate values ($N^* = 0.75$ and $N^* = 1.0$), the lateral spacing decreases, while, for high values ($N^* = 1.4$), the vortices move away from each other. This behavior was also observed, even more pronounced, for stratification without background turbulence[4].

Based on these results, an improvement of the simplified trajectory model proposed by Greene[12] is here proposed. In this model, one considers that the vortex altitude evolution is influenced by the self-induced velocity (Biot-Savart effect), $v_{BS}$, and by an additional vertical velocity due to the stratification, $v_{str}$:

$$\frac{d}{d\tau}\left(\frac{z}{b_0}\right) = \frac{v_{BS}}{V_0} + \frac{v_{str}}{V_0} \tag{26}$$

In order to compute the Biot-Savart component, one uses the measured maximum circulation on the results (see definition and computation below):

$$\frac{v_{BS}(\tau)}{V_0} = -\frac{\Gamma_{max}(\tau)}{\Gamma_0} \tag{27}$$

The additional stratification induced velocity is composed of two parts:

$$\frac{d}{d\tau}\left(\frac{v_{str}}{V_0}\right) = (\alpha_{str}\, N^*)^2 \left(\frac{z - z_0}{b_0}\right) - C\, \frac{v_{str}}{V_0} \tag{28}$$

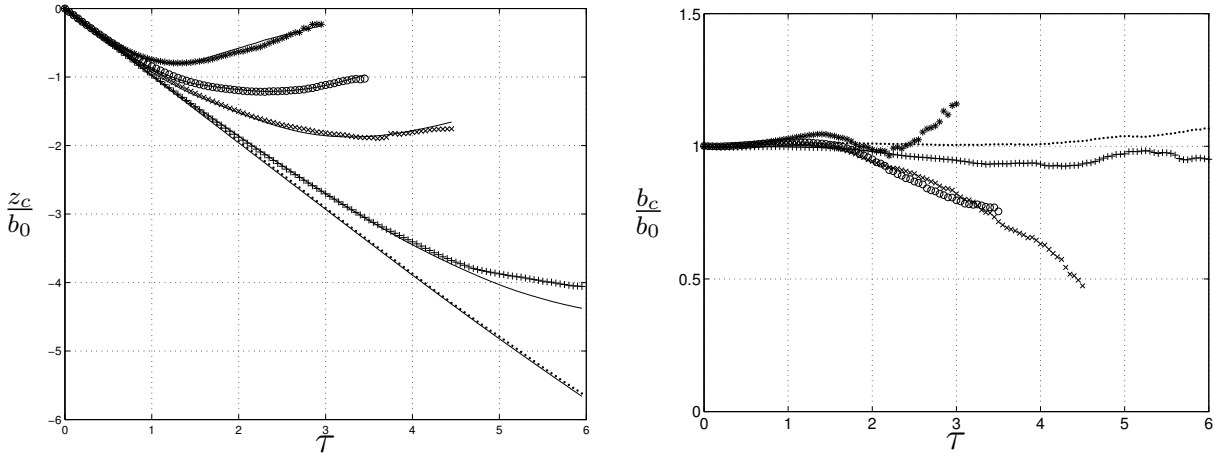


Figure 2: Time evolution of the vortex altitude (left) and lateral spacing (right): $N^* = 0.0$ ($\cdot$), $N^* = 0.35$ ($+$), $N^* = 0.75$ ($\times$), $N^* = 1.0$ ($\circ$) and $N^* = 1.4$ ($*$). For each stratification level, the results of a simplified model is also shown (solid lines).

The first term in Eq. (28) corresponds to that of Greene's model[12] and leads to a sinusoidal rebound controlled by the Brunt-Väisälä frequency. The second part is a damping term. This term has been added because the vorticity is diffused after a certain time leading to a decrease in the rebound. The second term is activated only for time $\tau \geq \tau_{crit}$. The model has been fitted on the numerical results. With $\alpha_{str} = 0.85$, $\tau_{crit} = 1.6$ and $C = 1.3$, this improved model is seen to fit very well the results for all cases. A small difference is observed between the results and the model for the case $N^* = 0.35$ for times $\tau \geq 5.0$. Recall that, for large aircraft at low altitudes, $\tau = 5.0$ would correspond to a time of roughly 150 s, which is already very long for ATM applications. This model will be implemented in operational models such as the DVM/PVM developed by UCL[13].

### 4.3 Circulation decay

A quantity of particular importance in wake vortex related hazards is the vortex circulation: the higher the circulation, the higher the induced rolling moment on a following aircraft. The circulation distribution $\overline{\Gamma}(r)$ is obtained by integration of the averaged axial vorticity component on a disk of radius r centered on the vortex centroid:

$$\overline{\Gamma}(r,t) = \int_0^{2\,\pi} \int_0^r \overline{\omega}_x(r',\theta,t)\, r'\, dr' d\theta\,. \tag{29}$$

A usual measurement of the vortex intensity is $\overline{\Gamma}_{5-15}$, which is an average of the circulation distribution, defined as

$$\overline{\Gamma}_{5-15}(t) = \frac{6}{b} \int_{\frac{b}{12}}^{\frac{b}{4}} \overline{\Gamma}(r,t) dr, \tag{30}$$

where $b = \frac{4}{\pi} b_0$ is the wingspan of the aircraft (assuming here an elliptical loading). This corresponds to what would come as post-processing of LIDAR measurements for a large aircraft (indeed taking $b = 60\,\mathrm{m}$, $\frac{b}{12} = 5\,\mathrm{m}$ and $\frac{b}{4} = 15\,\mathrm{m}$). To further characterize the wake vortices, we also examine the evolution of the maximum circulation, defined as

$$\overline{\Gamma}_{max}(t) = \max_r \overline{\Gamma}(r,t)\,. \tag{31}$$

This quantity is a good measure of the total circulation associated with the primary vortices.

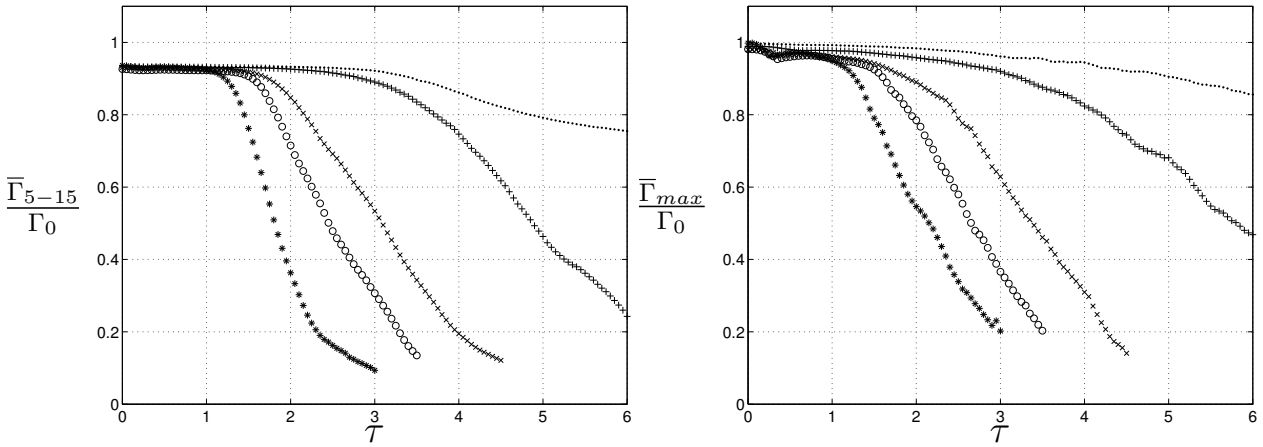


Figure 3: Time evolution of the vortex circulation $\overline{\Gamma}_{5-15}$(left) and $\overline{\Gamma}_{max}$: $N^* = 0.0$ ($\cdot$), $N^* = 0.35$ ($+$), $N^* = 0.75$ ($\times$), $N^* = 1.0$ ($\circ$) and $N^* = 1.4$ ($*$).

The time evolution of $\overline{\Gamma}_{5-15}$ and $\overline{\Gamma}_{max}$ are provided in Fig. 3. Using both circulation measurements, one observes two phases in the decay. During the first phase, there is almost no circulation decay. Later on, a second phase of rapid decay appears. The time at which this second phase appears depends on the stratification level.

The strong decay phase is caused by two phenomena. First, it is due to the 3-D interactions between the wake vortices and the turbulent baroclinic vorticity. The intensity of the baroclinic vorticity depends on the stratification level. Then, when the vortices come close to each other, 3-D interactions between the wake vortices themselves occur, which also enhances the circulation decay.

For the case with $N^* = 0.35$, the lateral spacing remains almost constant, the decay is thus mostly due to the baroclinic vorticity. The decay rate is thus the lowest. For the cases $N^* = 0.75$ and $N^* = 1.0$, $b_c$ decreases in time leading to an enhancement of the decay rate. Finally, for $N^* = 1.4$, the baroclinic vorticity intensity is very important but the vortices move away from each other, leading to little interaction between them. The net result is that, for the three highest stratification levels studied here, the decay rates are almost identical. It is also worth noting that, for $N^* = 1.4$, at $\tau \approx 3.0$, when the vortices are almost back at the generation altitude, the circulation is then very low:

$\overline{\Gamma}_{max} \approx 0.2\,\Gamma_0$. The encounter of such vortices would thus be much less hazardous than initially.

For the case without stratification, one observes a single phase of slow decay. Recall that the Crow instability cannot develop here since the axial extension of the periodical domain is $L_x = 4\,b_0$. The decay rate of the case without stratification is thus an upper bound of what to expect for vortices without Crow instabilities.

### 4.4 Sensitivity to the SGS model

In order to study the influence of the SGS model, a simulation was also performed, for the case $N^* = 1.0$, with more sophisticated SGS model, namely the RVMs model (see description above). A LES of the background turbulent stratified field was first performed. The wake vortex system evolving in this turbulent field was then simulated. Recall that, as we are at very high $Re$, the SGS is the only dissipation process possible in the simulation. Both SGS models used aim to dissipate energy only at small scales. Note also that the hyperviscosity model is numerically cheaper in a spectral code.

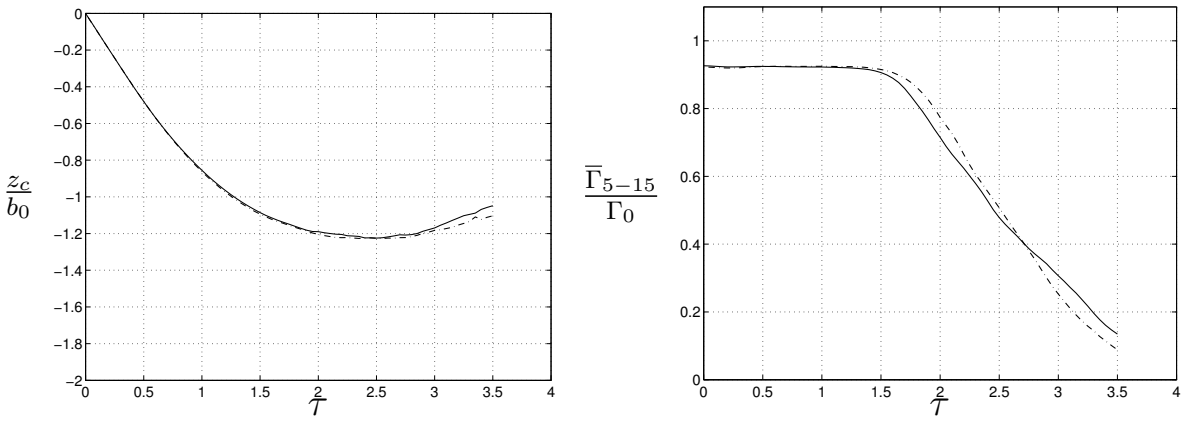


Figure 4: Time evolution of the vortex altitude (left) and circulation $\overline{\Gamma}_{5-15}$ (right) for the case $N^* = 1.0$ using, as SGS model, the hyperviscosity model (solid) or the RVMs model (dash dot).

Fig. 4 compares the altitude and $\overline{\Gamma}_{5-15}$ evolution of the wake vortices obtained using the two different SGS models. One observes that the use of either SGS models leads to very similar vortex behavior. Note also that, with both models, the circulation remains almost constant up to $\tau \approx 1.5$. This also confirms that both models don't dissipate until small scales are created. The hyperviscosity model is thus an appropriate model to be used for wake vortex application, also with stratification, in a spectral code.

### 4.5 Sensitivity to the domain size for the case $N^* = 1.0$

In order to study the influence of the domain size, a simulation was also performed, for the case $N^* = 1.0$, with a periodicity length of $8\,b_0$ with the same resolution (thus with $512^3$ grid points). A pre-simulation was also performed to obtain the background 3-D

stratified turbulence in the larger box. The turbulence contains thus larger scales that could enhance the development of large scale instabilities, such as the Crow instability, which has a wavelength of roughly $8\,b_0$.

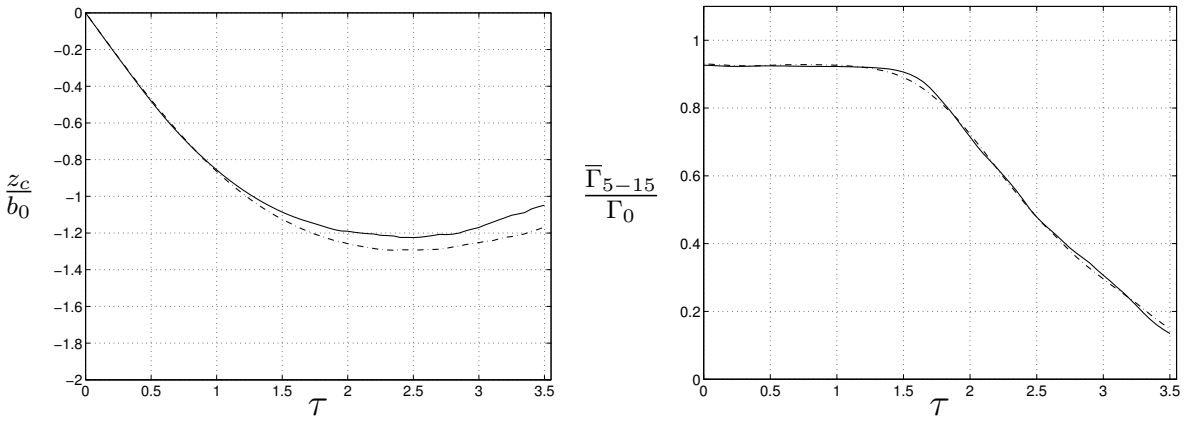


Figure 5: Time evolution of the vortex altitude (left) and circulation $\overline{\Gamma}_{5-15}$ (right) for the case $N^* = 1.0$ using a domain size of $4\,b_0 \times 4\,b_0 \times 4\,b_0$ (solid) or of size $8\,b_0 \times 8\,b_0 \times 8\,b_0$ (dash dot).

Fig. 5 compares the altitude and $\overline{\Gamma}_{5-15}$ evolution of the wake vortices obtained in the $(4\,b_0)^3$ and $(8\,b_0)^3$ domains. It appears that the size of the domain has no influence on the circulation decay and little influence on the vortex altitude evolution for the considered stratification level. As the stratification level is the same, it is not surprising that the rebound of the vortices are equivalent in both simulations. Moreover, since $N^* = 1.0$ is already quite high, the stratification effects dominate the circulation decay. It will lead to the creation of short wave instabilities (see Fig. 1), much shorter than $b_0$. This explains why large scale instabilities, such as the Crow instability, do not have time to develop.

### 4.6 Sensitivity to the background turbulence

In a previous work[4], LES of wake vortices in stably stratified fields were performed without background turbulence. The domain size was $b_0 \times 6\,b_0 \times 6\,b_0$ with the same resolution as the present simulations. A small random isotropic perturbation was added to the wake vortex velocity field, with a maximum amplitude set to $10^{-3}\,u_{\theta,max}$. Fig. 6 presents the comparison of the altitude and $\overline{\Gamma}_{5-15}$ evolution for three stratification levels, namely $N^* = 0.35$, $N^* = 1.0$ and $N^* = 1.4$.

One notices that the rebound is controlled by the stratification and not influenced by the background turbulence. For short times, the altitude evolutions thus correspond in both cases. The background stratified and weakly turbulent field has, on the other hand, a great influence on the development of the instabilities in the baroclinic vorticity and thus on the circulation decay of the vortices. Indeed, with background turbulence, the temperature field is turbulent, the baroclinic vorticity field is thus directly turbulent when created. The times of fast decay are thus shorter. As the stratification level increases,

the difference between the times of fast decay decreases. Nevertheless, the decay rate during the fast decay phase are identical with and without background turbulence. Since the circulation decays are different for late times, the altitude evolutions are obviously affected at those times and one can observe a difference in the trajectories.

## 5 CONCLUSIONS

We have performed numerical simulations of wake vortices interacting with a turbulent stably stratified atmosphere. In order to make those simulations as realistic as possible, we pre-computed five turbulent, stratified or not, fields by means of LES. We stress that those fields are not a superposition of a turbulent field and a stratified temperature field: they are obtained by LES of combined physics. In each of these fields, we then added a pair of wake vortices, using a realistic vortex model with relatively tight vortex cores. The Reynolds number was very high: much higher than in previous work, thus more realistic.

Visualizations of the flow were used to help understand the flow dynamics and relevant diagnostics were computed to analyze and compare the wake vortex behavior in the different atmospheric conditions.

As expected, the behavior is first essentially two dimensional. Then, tridimensional interactions between the primary vortices and the instabilities generated by the stratification strongly affect the trajectory and induce turbulence, and hence fast decay.

The stratification leads the vortices to rebound. The time of rebound is controlled by the stratification level. The stratification also influences the lateral displacement of the vortices. For low $N^*$ values, the lateral spacing of the vortices remains almost constant. For higher values ($N^* = 0.75$ and $N^* = 1.0$), the vortices come closer to each other. For $N^* = 1.4$, the vortices moves away from each other. A simplified trajectory model was also proposed and fitted on the altitude evolution. The model appears to be reliable for all stratification levels. This simplified model is of great interest for operational modeling.

Two phases are observed in the circulation decay. A fast decay phase follows a very slow decay phase. The starting time of this rapid decay is a function of the stratification level. Two decay mechanism act in this rapid decay phase. First the wake vortices interact with the turbulent baroclinic vorticity. In addition, when the vortices are brought close to each other (case $N^* = 0.75$ and $N^* = 1.0$), 3-D interactions also appear between the two vortices themselves. In both cases, at late stages of the flow, the baroclinic secondary vorticity is mixed, leading to the creation of complex turbulent structures surrounding the primary vortices and then strongly interacting with them (in fact also leading to short wave instabilities developing in the vortex cores).

The influence of the domain size was also studied for the case $N^* = 1.0$. It appeared that for such high stratification levels, the physics are essentially governed by short waves instabilities. The axial extension of the domain thus had no significant effect. However, for low stratification levels, the Crow instability could appear and an axial extension of the domain up to $8\,b_0$ would then be required.

We also compared the behavior of wake vortices evolving in stratified atmosphere with

and without weak ambient turbulence. It appeared that the turbulent nature of the temperature field has a weak influence on the vortex rebound, which is mainly governed by buoyancy. On the contrary, the effect on the circulation decay is very high. Indeed, the baroclinic vorticity generated around the primary vortices is directly turbulent and thus sooner unstable. These instabilities grow in time and the baroclinic vorticity interacts with the wake vortices leading to a fast decay of their circulation. The decay rate of the fast decay phase is thus essentially identical, with and without background turbulence, but the time of fast decay is different.

The stratification is a very efficient mechanism to destroy wake vortices, and even more so when combined with weak ambient turbulence, as is always the case in the real atmosphere. This fact is of great importance from an operational point of view. The present results also are of great importance for the further improvement and calibration of the operational wake vortex models.

## 6 Acknowledgments

The simulations were done using the facilities of the Calcul Intensif et Stockage de Masse (CISM) on the UCL Lemaître cluster funded by Fonds National de Recherche Scientifique (FNRS) under a FRFC Project and by UCL (Fonds Spéciaux de Recherche). Part of the results were obtained in the framework of the research projects Green-Wake and WakeNet3-Europe funded by the European Commission (FP7).

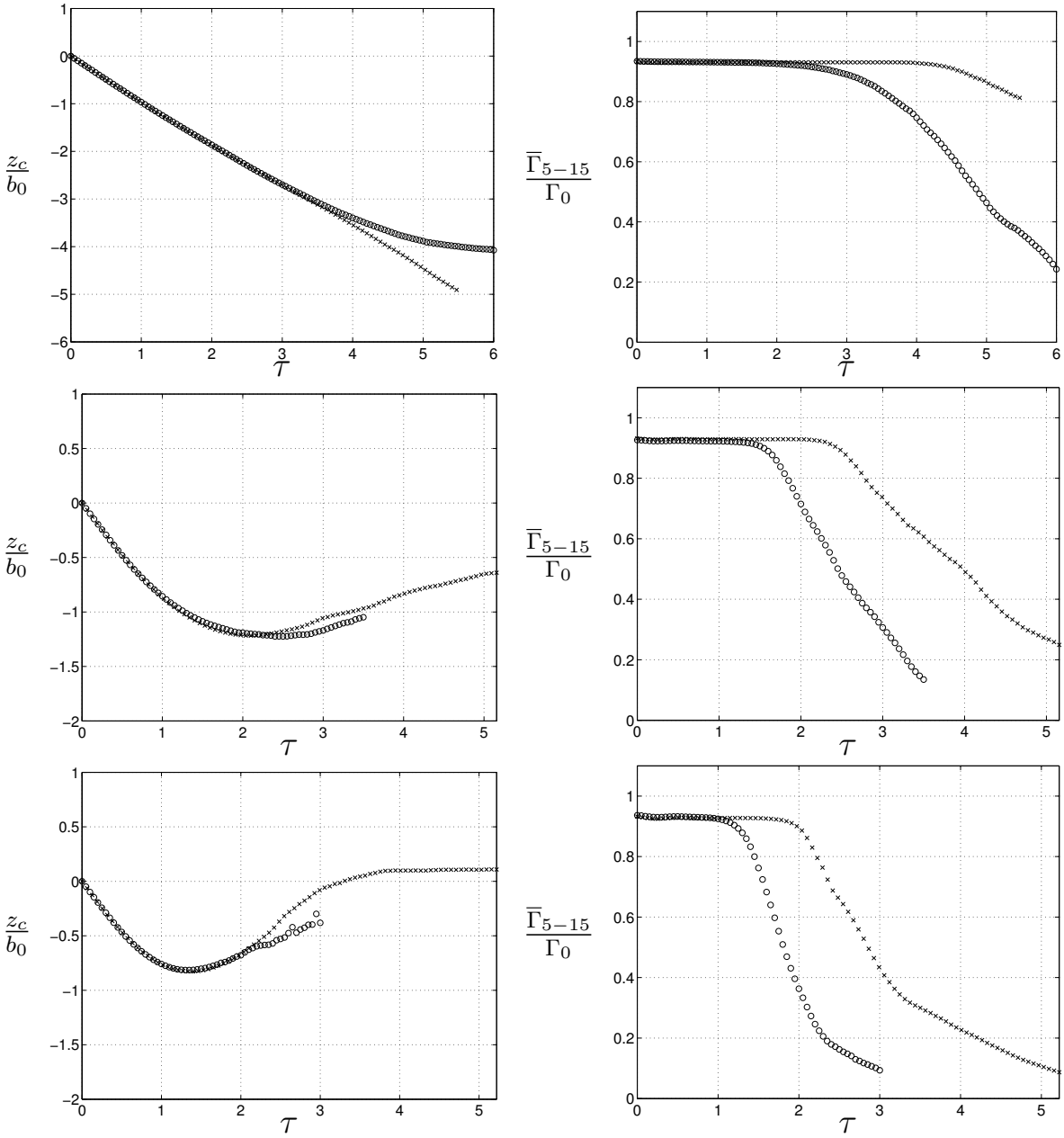


Figure 6: Time evolution of the vortex altitude (left) and circulation $\overline{\Gamma}_{5-15}$ (right) for $N^* = 0.35$ (top), $N^* = 1.0$ (middle) and $N^* = 1.4$ (bottom) for a case with weak background turbulence ($\circ$) and without ($\times$).

## REFERENCES

[1] F. Holzäpfel and T. Gerz, Two-dimensional wake vortex physics in the stably stratified atmosphere, *Aerospace Science and Technology*, **Vol. 3**, 261–270 (1999).

[2] F. Holzäpfel, T. Gerz and R. Baumann, The turbulent decay of trailing vortex pairs in stably stratified environments, *Aerospace Science and Technology*, **Vol. 5**, 95–108 (2001).

[3] K. K. Nomura, H. Tsutsui, D. Mahoney and J. W. Rottman, Short-wavelength instability and decay of a vortex pair in a stratified fluid, *Journal of Fluid Mechanics*, Cambridge University Press, **Vol. 553**, 283–322 (2006).

[4] I. De Visscher, L. Bricteux, G. Winckelmans, S. Caliaro and T. Vilbajo, Large Eddy Simulations of aircraft wake vortices in a stably stratified atmosphere, In proceedings of the *Sixth International Symposium on Turbulent and Shear Flow Phenomena*, TSFP-6, Seoul National University, Korea (2009)

[5] C. Canuto, M. Y. Hussaini, A. Quarteroni and T. A. Zang, Spectral Methods in Fluid Dynamics, *Springer-Verlag*, New-York (1988).

[6] R. Cocle, L. Dufresne, and G. Winckelmans, Investigation of multiscale subgrid models for LES of instabilities and turbulence in wake vortex systems, *Complex Effects in LES: Springer volume*, LNCSE series (2006).

[7] L. Bricteux, R. Cocle, M. Duponcheel, L. Georges and G. Winckelmans, Assessment of multiscale models for LES: spectral behavior in very high Reynolds number turbulence and cases with aircraft wake vortices, In proceedings of the *Fifth International Symposium on Turbulence and Shear Flow Phenomena*, TSFP5, **Vol. 1**, 327–331 ,TU München, Garching, Germany (2007).

[8] Jeanmart H. and Winckelmans G., Investigation of eddy-viscosity models modified using discrete filters: a simplified "regularized variational multiscale model" and an "enhanced field model", *Phys. Fluids*, **Vol. 19**(5), 055110 (2007).

[9] R. Cocle, L. Bricteux, and G. Winckelmans, Scale dependence and asymptotic very high Reynolds number spectral behavior of multiscale subgrid models, *Phys. Fluids*, **Vol. 21**, 085101 (2009).

[10] L. Bricteux, M. Duponcheel, and G. Winckelmans, A multiscale subgrid model for both free vortex flows and wall-bounded flows, *Phys. Fluids*, **Vol. 21**(5), 105102 (2009).

[11] J. Jeong and F. Hussain, On the identification of a vortex, *J. Fluid Mech.*, **Vol. 285**, 69–94 (1995).

[12] G. C. Greene, An Approximate model of vortex decay in atmosphere, *Journal of Aircraft*, **Vol. 23**, 566–573 (1986).

[13] G. Winckelmans, Overview of UCL operational tools for predicting aircraft wake vortex transport and decay: the Deterministic/Probabilistic wake Vortex Models (DVM/PVM) and the WAKE4D platform, *Technical report*, Université catholique de Louvain (UCL) (2009).